Atmospheric
Chemistry
and Physics

Photochemical processing of aqueous atmospheric brown carbon

R. Zhao[1], **A. K. Y. Lee**[1], **L. Huang**[2], **X. Li**[3], **F. Yang**[4], and **J. P. D. Abbatt**[1]

[1]Department of Chemistry, University of Toronto, 80 St. George Street, Toronto, ON, Canada
[2]Climate Research Division/Atmospheric Science and Technology Directorate/Science and Technology
Branch, Environment Canada, Toronto, Canada
[3]School of Chemistry and Environment, Beihang University, Beijing, China
[4]Chongqing Institute of Green and Intelligent Technology, Chongqing, China

Correspondence to: J. P. D. Abbatt (jabbatt@chem.utoronto.ca)

Abstract. Atmospheric brown carbon (BrC) is a collective term for light absorbing organic compounds in the atmosphere. While the identification of BrC and its formation mechanisms is currently a central effort in the community, little is known about the atmospheric removal processes of aerosol BrC. As a result, we report on a series of laboratory studies of photochemical processing of BrC in the aqueous phase, by direct photolysis and OH oxidation. Solutions of ammonium sulfate mixed with glyoxal (GLYAS) or methylglyoxal (MGAS) are used as surrogates for a class of secondary BrC mediated by imine intermediates. Three nitrophenol species, namely 4-nitrophenol, 5-nitroguaiacol and 4-nitrocatechol, were investigated as a class of water-soluble BrC originating from biomass burning. Photochemical processing induced significant changes in the absorptive properties of BrC. The imine-mediated BrC solutions exhibited rapid photo-bleaching with both direct photolysis and OH oxidation, with atmospheric half-lives of minutes to a few hours. The nitrophenol species exhibited photo-enhancement in the visible range during direct photolysis and the onset of OH oxidation, but rapid photo-bleaching was induced by further OH exposure on an atmospheric timescale of an hour or less. To illustrate the atmospheric relevance of this work, we also performed direct photolysis experiments on water-soluble organic carbon extracted from biofuel combustion samples and observed rapid changes in the optical properties of these samples as well. Overall, these experiments indicate that atmospheric models need to incorporate representations of atmospheric processing of BrC species to accurately model their radiative impacts.

1 Introduction

There is increasing awareness of the importance of light absorbing organic compounds in the atmosphere (Kirchstetter et al., 2004; Chen and Bond, 2010; Lack et al., 2012; Bahadur et al., 2012; Laskin et al., 2015). Highly variable in sources and identity, this class of poorly characterized organic compounds has been collectively termed atmospheric brown carbon (BrC; Andreae and Gelencser, 2006). BrC significantly alters the traditional view that organic carbon interacts with solar radiation via scattering only (Chung and Seinfeld, 2002). In the visible range of solar radiation, BrC absorption can affect the direct radiative effect of organic carbon (Feng et al., 2013; Lin et al., 2014; Liu et al., 2014). In particular, Feng et al. (2013) have shown that defining a fraction of organic aerosol as strongly light-absorbing BrC in a global chemical transport model can shift the direct radiative effect of organic carbon from net cooling to net warming. Meanwhile, in the near-UV range, BrC absorption may affect the flux of short-wavelength radiation that is crucial for driving atmospheric photochemistry (Jacobson, 1999). Motivated by such atmospheric impacts, the characterization of the sources, molecular identity and processing of BrC is a central effort in the aerosol chemistry community.

Atmospheric BrC arises from multiple sources, including primary emission from biomass burning (BB; Andreae and Gelencser, 2006; Alexander et al., 2008; Chen and Bond, 2010; Lack et al., 2012; Kirchstetter and Thatcher, 2012; Saleh et al., 2014), as well as anthropogenic emissions (Bond, 2001; Zhang et al., 2011). Recently, BB has been reported as the dominant source of BrC observed at a

location in the southeastern US (Washenfelder et al., 2015). The chemical composition of BB organic aerosol is highly complex, and the optical properties of BB organic aerosol also vary significantly with source fuels and burning conditions (Chen and Bond, 2010). Such complexity significantly hinders the separation, analyses, and molecular identification of BB BrC. BB BrC is at times considered to belong to humic-like substances (HULIS; Hoffer et al., 2004; Graber and Rudich, 2006) and more recently a class of compounds categorized as extremely low volatility organic compounds (Saleh et al., 2014). Nitrophenols represent a class of speciated BrC species in BB plumes (Vione et al., 2009; Einschlag et al., 2009) and have often been employed as molecular tracers for BB (Iinuma et al., 2010; Kitanovski et al., 2012). However, the contribution of nitrophenols to the total absorption of BB BrC is small, with the majority of organic chromophores unspecified (Mohr et al., 2013; Desyaterik et al., 2013).

Secondary formation of BrC in the atmospheric aqueous phases (i.e., cloud, fog and aerosol liquid water) has also been proposed. Photooxidation of aromatic compounds in the aqueous phase gives rise to colored organic compounds with absorption spectra similar to those of HULIS (Chang and Thompson, 2010; Gelencser et al., 2003). Recently, a type of BrC arising from aldehydes reacting with nitrogen containing nucleophiles (e.g., ammonia, amines and amino acids) has been investigated extensively in the laboratory (Bones et al., 2010; De Haan et al., 2009, 2010; Shapiro et al., 2009; Noziere et al., 2009; Sareen et al., 2010; Yu et al., 2011; Zarzana et al., 2012; Kampf et al., 2012; Sedehi et al., 2013; Powelson et al., 2013; Updyke et al., 2012; Nguyen et al., 2013; Laskin et al., 2014; Flores et al., 2014). Since the formation mechanism of this type of BrC involves an imine or a Schiff's base intermediate, this class of BrC is herein referred to as "Imine BrC". Although imine intermediates do not absorb at the actinic range, they undergo subsequent reactions to form nitrogen-containing organic chromophores (Lee et al., 2013; Kampf et al., 2012; Yu et al., 2011). It is generally believed that formation of individual chromophores with very low concentrations leads to the color (Nguyen et al., 2013). Imine BrC typically takes days to form in the bulk laboratory solution (Noziere et al., 2009; Shapiro et al., 2009; Sareen et al., 2010; Lee et al., 2013). However, studies have also shown that droplet evaporation may significantly accelerate the rate of such reactions, giving rise to rapid formation of BrC (De Haan et al., 2010; Zarzana et al., 2012; Nguyen et al., 2012; Lee et al., 2013; Galloway et al., 2014). While Imine BrC has received an enormous amount of attention from laboratory studies, it has not been reported in ambient measurements.

Finally, we note that a recent study has also suggested that charge transfer complexes between different functional groups may be responsible for absorption in the visible range (Phillips and Smith, 2014). We did not perform experiments targeted at this potential third class of BrC species.

Studies from the past decade (Blando and Turpin, 2000; Ervens et al., 2011) have indicated atmospheric aqueous phases (e.g., cloudwater and aerosol liquid water) as important reaction media, where organic compounds can be processed, leading to formation and further aging of secondary organic aerosol (SOA). Imine BrC, forming in the aqueous phase, can undergo subsequent photochemical processing. A previous study has observed rapid photolysis of components in the mixture of methylglyoxal and ammonium sulfate, implying rapid photolysis of Imine BrC (Sareen et al., 2013). More recently, Lee et al. (2014b) investigated aqueous-phase processing of several classes of BrC and observed rapid decay of color (photo-bleaching). To date, there has been no systematic investigation of the effect of OH oxidation on Imine BrC. BB BrC, on the other hand, can also be subject to aqueous-phase photochemical processing, given that BB particulate matter can be hygroscopic (Petters and Kreidenweis, 2007; Petters et al., 2009) and that a significant fraction of BB BrC belongs to water-soluble organic carbon (WSOC; Iinuma et al., 2007; Chen and Bond, 2010; Zhang et al., 2011, 2013; Washenfelder et al., 2015). In particular, Zhong and Jang (2014) have recently observed changing optical properties of BB particles during photochemistry in chamber experiments, with more rapid changes observed under higher relative humidity.

As the ambient BrC is highly complex in nature, investigating the behavior of surrogate compounds or mixtures of BrC in the laboratory with reduced complexity can be highly valuable. In this study, nitrophenols are chosen as surrogates for BB BrC species. Certain nitrophenols exhibit relatively high Henry's law constants (Schwarzenbach et al., 1988) and have been observed from cloudwater samples (Luttke and Levsen, 1997; Luttke et al., 1999; Harrison et al., 2005; Desyaterik et al., 2013); hence, their aqueous-phase chemistry can be highly relevant to the atmosphere. Previous studies have investigated aqueous-phase UV photolysis (Chen et al., 2005; Zhao et al., 2010), OH oxidation (Einschlag et al., 2003, 2009; Vione et al., 2009), as well as heterogeneous oxidation (Knopf et al., 2011; Slade and Knopf, 2014) of nitrophenols, but a clear connection to their optical properties has not been made. For surrogates of Imine BrC, solutions of glyoxal or methylglyoxal mixed with ammonium sulfate are chosen because the precursor compounds are highly relevant to atmospheric aqueous phases, and this type of Imine BrC has been investigated by previous studies (see references listed previously).

In this study, we systematically investigate how atmospheric photochemical processing mechanisms affect Imine BrC and nitrophenols (as surrogates of BB BrC) in the aqueous phase, focusing on changes in their absorptive optical properties. The dual objectives are (1) to quantify the rates of direct photo-bleaching and/or photo-enhancement under realistic radiation condition, and (2) to evaluate the atmospheric importance of BrC oxidative processing, with a particular focus on OH oxidation. We perform these experiments
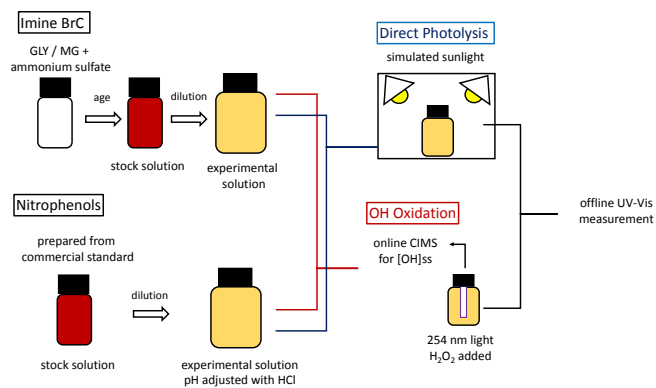
Figure 1. Experimental procedures.

quantitatively under known light and OH exposures, so as to establish which processing mechanism is likely to dominate in the atmosphere. To tie our laboratory experiments to ambient conditions, we also performed direct photolysis experiments on the WSOC extracted from biofuel combustion particles.

2 Experimental

2.1 Preparation of BrC solutions

The experimental procedures for Imine BrC and nitrophenols are illustrated in Fig. 1. Solutions of ammonium sulfate mixed with glyoxal (GLYAS) or methylglyoxal (MGAS) were chosen as laboratory surrogates to represent Imine BrC. Stock solutions (200 mL in volume) were made by mixing ammonium sulfate (1.5 M, Sigma Aldrich) with either 0.5 M of glyoxal (Sigma Aldrich, 30 % in water) or 0.2 M of methylglyoxal (Sigma Aldrich, 40 % in water) in 250 mL glass jars. All the solutions were prepared using deionized water (18 mΩ-cm) with total organic carbon less than 1 parts per billion (ppb). The stock solutions were sealed and placed in the dark under room temperature for 2 to 3 months. During this time, the color of the solutions turned dark yellow and eventually dark brown, consistent with previous studies (Shapiro et al., 2009; Sareen et al., 2010; Lee et al., 2013). Although 2 to 3 months is much longer than typical atmospheric aerosol lifetimes, our previous work has shown that the absorption spectra of Imine BrC obtained this way closely resembled those obtained from droplet evaporation occurring on the timescales of seconds or less (Lee et al., 2013). The experimental solutions were created by diluting the concentrated stock solutions, typically by a factor of 200, to concentrations that optimize the UV-Vis detection at 400 nm (see next section).

Three nitrophenol compounds (4-nitrophenol (4NP), 5-nitroguaiacol (5NG) and 4-nitrocatechol (4NC)) were chosen to represent primary BB BrC (structures shown in Fig. 2) and are investigated individually. 4NP and 4NC have been
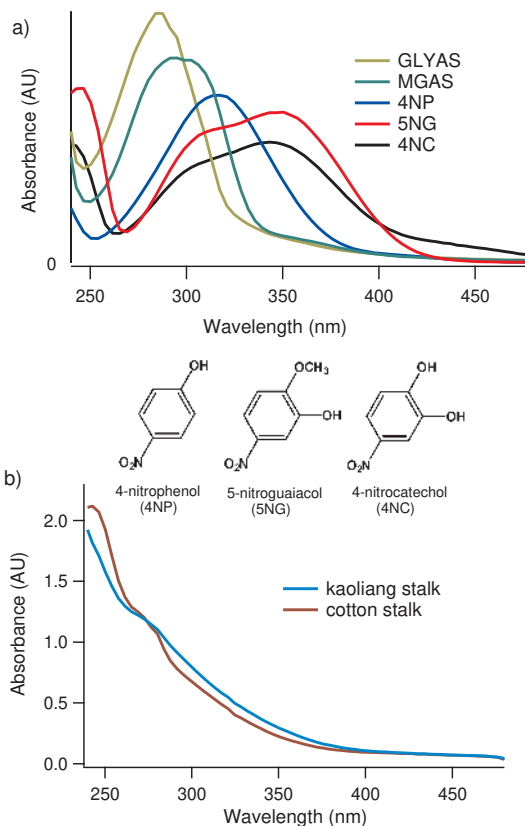

Figure 2. Absorption spectra of BrC investigated in this study (**a**) and WSOC from the biofuel combustion samples (**b**). The *y* axis in (**a**) is in arbitrary units to keep the absorbance of all the solutions on scale.

detected from BB affected cloudwater samples (Desyaterik et al., 2013), while 5NG has been previously used in the laboratory as a model compound for BB organic matter (Knopf et al., 2011). Commercial standards of these compounds were purchased from Sigma Aldrich and were used without further purification. Individual stock solutions (1 mM) were created every few days, and the experimental solutions were made by diluting the stock solution to 4 to 15 μM depending on the nitrophenol species and the type of experiment. This range of concentration matches that of nitrophenols detected in cloudwater (Desyaterik et al., 2013).

2.2 Direct photolysis and OH oxidation experiments

Direct photolysis and OH oxidation experiments were conducted separately (Fig. 1). Direct photolysis experiments were performed with a Suntest CPS photo-simulator (Atlas) equipped with a Xe lamp. The BrC solution (100 mL) contained in a glass bottle was placed inside the simulator for illumination. Chemical actinometry using 2-nitrobenzaldehyde (Galbavy et al., 2010) was performed to measure the effective photon flux, which was determined to be similar to actinic flux at the Earth's surface with 0 °C

zenith angle. The method of chemical actinometry and the determined photon flux from the simulator are included in Sect. S1 in the Supplement. Aliquots of the experimental solution were taken at different illumination times for offline absorption measurements conducted by a liquid waveguide capillary UV-Vis spectrometer (World Precision Instruments), equipped with a deuterium tungsten halogen light source (DT-Mini-2, Ocean Optics) and a temperature controlled UV-Vis spectrometer (USB2000+, Ocean Optic). The strength of this instrument lies in its long effective optical length (50 cm in this work), resulting in its superior detection sensitivity. The spectrometer simultaneously records absorption from 230 to 850 nm, making monitoring at multiple wavelengths possible. We confirmed that the concentrations of the experimental solutions were in the linear range of the spectrometer used.

Experiments for OH oxidation were conducted in a different setup. Hydrogen peroxide (H_2O_2, TraceSELECT 30 % purchased from Sigma Aldrich) was added to each solution as a photolytic source of OH radical upon irradiation with a 254 nm mercury lamp (UVP, an ozone-free version constructed to remove the 185 nm line) inserted inside the solution. The BrC solutions were prepared in the same manner but in a larger volume (1 L). The concentration of H_2O_2 added to the BrC solutions was typically 5 mM unless otherwise stated. H_2O_2 itself exhibited UV absorption up to 300 nm, but did not affect BrC absorption at longer wavelengths. Dark control experiments were also performed to confirm that H_2O_2 did not react with BrC to change its optical properties. Aliquots of offline samples were taken at different illumination times and were measured by the liquid waveguide capillary UV-Vis spectrometer as mentioned above.

It is crucial to measure the steady state concentration of OH radicals ([OH]ss) in the OH oxidation experiments in order to make sound environmental implications. An aerosol chemical ionization mass spectrometer (Aerosol-CIMS) was employed for this purpose. The experimental setup is similar to that in one of our previous studies (Zhao et al., 2012). Briefly, the experimental solution is constantly atomized with a TSI constant output atomizer (model 3076). The aerosol flow is introduced through a heated metal line (100 °C), where organic compounds volatilize to the gas phase and are detected by a quadruple CIMS equipped with an iodide water cluster reagent ion ($I(H_2O)_n^-$). The $I(H_2O)_n^-$ reagent ion detects oxygenated organic compounds by forming iodide ion clusters (Aljawhary et al., 2013; Lee et al., 2014a; Zhao et al., 2014). The [OH]ss was estimated by tracking the pseudo first-order decay of a reference compound with known OH reactivity. For the Imine BrC, unreacted glyoxal or methylglyoxal in the solutions was used as the tracer compound because their mono-hydrates are detectable by the $I(H_2O)_n^-$ reagent ion (Zhao et al., 2012). The OH oxidation rate constants of glyoxal and methylglyoxal used in this study are $1.1 \times 10^6 \, M^{-1} \, s^{-1}$ (Tan et al., 2009) and $5.3 \times 10^8 \, M^{-1} \, s^{-1}$

(Monod et al., 2005), respectively. For the nitrophenols, as the iodide reagent ion does not detect nitrophenol species, 1 mM of meso-erythritol (Sigma Aldrich) was added to the solution as the reference compound. The choice of erythritol is based on the fact that (1) it does not absorb light in the actinic wavelength, (2) it is not an acid and does not affect the solution pH, and (3) it reacts with OH rapidly, with a second-order rate constant of $1.9 \times 10^9 \, M^{-1} \, s^{-1}$ (Hoffmann et al., 2009).

2.3 Direct photolysis of WSOC from biofuel combustion

The biofuel combustion samples were collected in Henan Province, China (Li et al., 2007, 2009). Agricultural residues, typically used as biofuels in the local area, were burned in an improved stove commonly used in the area. A detailed description of particle collection and the physical properties of the generated particles are provided in Li et al. (2007). Briefly, particles were withdrawn from the stove, and the $PM_{2.5}$ fraction was collected on quartz filters after dilution. The quartz filters were baked under 450 °C before collection, and the samples were stored frozen after collection. Organic carbon (OC) and elemental carbon contents of each filter sample were measured following a method originally developed at the Environment Canada's laboratory in Toronto for measuring $\delta^{13}C$ of OC/EC (Huang et al., 2006) and later improved by Chan et al. (2010) to be used as the standard OC/EC measurements in the aerosol baseline measurements in Canada. In the current work, we investigated the WSOC from two filter samples, collected from burning of kaoliang stalks and cotton stalks, respectively. A quarter of the filter was extracted in 10 mL of deionized water by constant shaking for 30 min. The extracts were used as the experiment solution after filtration with a 0.2 µm syringe filter. We extracted the same filter a second time and found that the absorption in the second extract was less than 10 % of the first extract. However, it is difficult to estimate the extraction efficiency of total organic carbon. The filtered extract was illuminated with the same solar simulator, and its absorption was monitored with the same waveguide capillary spectrometer mentioned in Sect. 2.2. Oxidation by OH radicals was not performed for these samples due to a limited amount of sample volume.

3 Results and discussion

3.1 Light absorption by BrC

Absorption spectra of the BrC solutions are displayed in Fig. 2a. The concentrations of the solutions were chosen to display their full absorption spectra up to 480 nm. The absorption spectra of all of these species stretch into the visible range of radiation, giving a brown to light yellow color to the solutions. Absorption spectra of the two WSOC extracts

from biofuel combustion samples are shown in Fig. 2b. Absorption with strong wavelength dependence was observed, with Angstrom absorption coefficients (290 to 480 nm) of 6.0 and 5.8 for the kaoliang stalk and cotton stalk samples, respectively. We note that the absorption spectra of the individual BrC species do not resemble those of the biofuel sample extracts, as such ambient samples likely contain a large number of BrC with various absorptivities. Investigation of the selected Imine BrC and nitrophenol species in this study is intended to provide fundamental information for processing of individual BrC species.

To provide more quantitative values, we also obtained the wavelength-dependent mass absorption coefficient (MAC) for the Imine BrC and biofuel combustion samples (see Sect. S2). The MAC of the Imine BrC solutions was calculated based on its total organic carbon content measured by a Shimadzu TOC-ICPH total organic carbon analyzer. The MAC of the biofuel combustion samples was calculated based on its organic carbon contents measured in the filter samples. For nitrophenols, we obtained their absorption coefficient and molar absorptivity instead of MAC, because they are single compounds. The detailed methods and complete results are shown in Sect. S2. We note that the MAC values reported are for the bulk solutions and not for particles, and are obtained by dividing the bulk absorption coefficient by the material density (Sect. S2.1).

3.2 Imine BrC

3.2.1 Direct photolysis of Imine BrC

Both the GLYAS and MGAS solutions exhibited rapid photo-bleaching upon illumination by simulated sunlight. Figure 3a shows the spectral change of one MGAS solution as an example, with the illumination time color-coded. Absorbance over the entire spectral range exhibited uniform decay during 2 h of illumination. In Fig. 3b, we show the time profiles of absorbance at 400 nm normalized to its initial value at $t = 0$ for both the GLYAS and MGAS solutions. The wavelength of 400 nm was chosen because the concentrations of the Imine BrC solutions were optimized for the detection at this wavelength. The inset displays the first-order plots for the decay, along with the fitted linear lines forced through the origin. The nonlinear plots indicate non-first-order behavior, likely due to the presence of multiple chromophores that exhibit different degrees of photo-lability.

Aregahegn et al. (2013) proposed that photosensitized reactions take place in the GLYAS solution, initialized by compounds such as imidazole and imidazole–carboxaldehyde. We examined the presence of this type of reaction by varying the initial concentration of the Imine BrC. However, the concentration of Imine BrC did not affect its photolysis rate constant (Sect. S3). This indicates that photosensitized reactions either did not take place in our reaction system, or were not indicated by the color change.
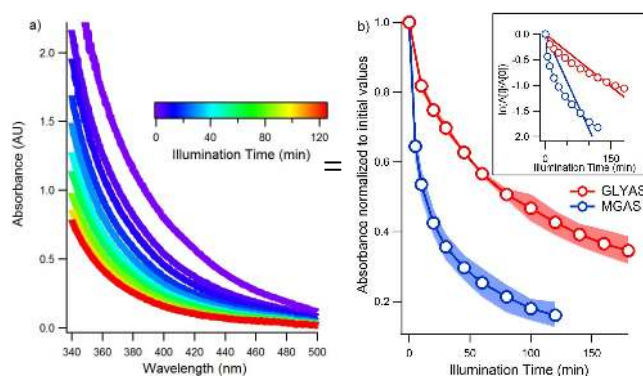

Figure 3. Spectral change of the MGAS solution during a direct photolysis experiment **(a)** and the absorbance change at 400 nm as a function of illumination time **(b)**. The inset in **(b)** shows the first-order plot of the decay, and the lines are linear least square plots forced through the origin. The shaded areas represent the range obtained from three replicates.

3.2.2 OH oxidation of Imine BrC

Rapid photo-bleaching was observed also during the OH oxidation experiments. Figure 4a shows the evolution of absorbance at 400 nm during four experiments, normalized to the values at the beginning of illumination. The dashed lines are H_2O_2 control experiments, where the absorbance at 400 nm for both GLYAS and MGAS exhibited decay due to direct photolysis by the 254 nm lamp. The decay was clearly accelerated during OH oxidation experiments represented by the solid line traces. The calculated [OH]ss values in these two experiments were 9×10^{-14} and 1×10^{-13} M for the GLYAS and MGAS experiments, respectively.

The decay of absorbance at 400 nm appeared largely pseudo first order, except for the GLYAS OH oxidation (Fig. 4b). Similar to the case of direct photolysis, we suspect that multiple chromophores likely give rise to the non-first-order decay of the color. We have decided to treat the decay in the GLYAS system as if it were pseudo first order, with the rates determined this way representing the middle point between the fastest and slowest decay rates.

Assuming the difference between the H_2O_2 control and the OH oxidation experiments is due to OH oxidation, a pseudo first-order OH oxidation rate constant (k_{OH}^I) can be obtained by taking the difference between the observed pseudo first-order decay of absorbance in the H_2O_2 control (k_{ctl}^I) and the OH oxidation experiments (k_{oxi}^I), as shown by Eq. (1). The second-order OH oxidation rate constant (k_{OH}^{II}) can then be calculated from Eq. (2).

$$k_{OH}^I = k_{oxi}^I - k_{ctl}^I \tag{1}$$
$$k_{OH}^{II} = k_{OH}^I/[OH]ss \tag{2}$$

As listed in Table , the k_{OH}^{II} values for the GLYAS and MGAS systems are determined to be $(2.1 \pm 1.1) \times 10^{10}$ and $(1.2 \pm$
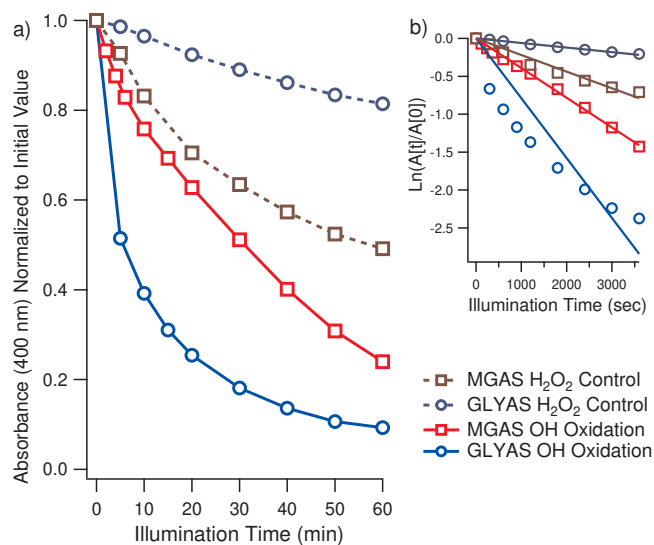
Figure 4. Time profiles of absorbance at 400 nm during OH oxidation (solid lines) and H_2O_2 control (dashed lines) experiments. Results for both the GLYAS (blue traces) and MGAS (red traces) solutions are shown. The decay profiles of absorbance at 400 nm normalized to the initial value at $t = 0$ are shown in **(a)**, while their corresponding first-order decay plots are shown in **(b)**.

$0.3) \times 10^9 \, M^{-1} \, s^{-1}$, respectively. The uncertainty represents SD from between three and four experimental replicates. We note that the k_{OH}^{II} value for the GLYAS system is essentially diffusion limited.

3.2.3 Atmospheric fate of Imine BrC

We estimate the atmospheric half-life ($\tau_{1/2}$) of Imine BrC against direct photolysis and aqueous-phase OH oxidation based on the observed absorbance change at 400 nm (Table). The $\tau_{1/2}$ values were obtained by extracting the time when the signal reached half of its original value, and the uncertainty represents the range obtained from three replicates. Since the photon flux in the solar simulator is similar to that in the ambient atmosphere (see Sect. S1), the experimentally determined $\tau_{1/2}$ values, 90 ± 12 and 13 ± 3 min for the GLYAS and MGAS systems, directly reflect the photolytic $\tau_{1/2}$ of these Imine BrC species in the ambient atmosphere. These $\tau_{1/2}$ values are on the same order as another type of Imine BrC generated from Limonene SOA and ammonia vapor (Lee et al., 2014b), implying that rapid photolysis will be a common characteristic for this type of BrC. The OH oxidation half-lives are estimated by assuming an ambient cloudwater [OH]ss of 1×10^{-13} M, which represents the upper band of OH in remote cloudwaters (Herrmann et al., 2010). This [OH]ss, together with the k_{OH}^{II} determined in the previous section (Sect. 3.2.2), yields OH oxidation $\tau_{1/2}$ of 5 and 98 min for the GLYAS and the MGAS solutions, respectively. The rapid bleaching implies that the daytime lifetime of Imine BrC is likely very short in the atmosphere, lead-

Table 1. Estimated atmospheric half-life ($\tau_{1/2}$) of Imine BrC arising in the glyoxal–ammonium sulfate (GLYAS) and methylglyoxal–ammonium sulfate (MGAS) solutions.

	Photolytic $\tau_{1/2}$ (min)	k_{OH}^{II} ($M^{-1}\,s^{-1}$)	OH $\tau_{1/2}$ (min)
GLYAS	90 ± 12	$2.1\,(\pm1.1) \times 10^{10}$	5
MGAS	13 ± 3	$1.2\,(\pm0.3) \times 10^{10}$	98

ing to relatively low concentrations. Knowing that droplet evaporation can lead to rapid formation of Imine BrC on a timescale of seconds (Lee et al., 2013), its steady state concentration may be highest where droplet evaporation processes are occurring at night.

Although Imine BrC in the GLYAS and MGAS solutions is thought to be arising from similar reaction mechanisms (De Haan et al., 2010; Yu et al., 2011; Sedehi et al., 2013), their major bleaching processes are found to be different. The GLYAS solution is predominantly bleached by OH oxidation, while the MGAS solution is by direct photolysis. The results for the MGAS solution show agreement with Sareen et al. (2013), where they determined direct photolysis as the dominant sink for constituents in the MGAS solution. To our best knowledge, the current work presents the first investigation for direct photolysis of GLYAS, as well as the OH oxidation kinetics for both GLYAS and MGAS.

The difference in the major removal mechanisms for GLYAS and MGAS arises from the additional methyl group on methylglyoxal as compared to glyoxal, as we propose in Fig. 5. The methyl group prevents the carbonyl functionality from hydrating into its geminal diol, which does not absorb actinic radiation. On the other hand, H-abstraction from a methyl hydrogen is expected to be slower than from the tertiary hydrogen on the geminal diol. In Fig. 5, we use imidazole–carboxaldehyde, proposed as a major product in the GLYAS solution (Kampf et al., 2012; De Haan et al., 2010; Yu et al., 2011), as an example to demonstrate this concept.

3.3 Nitrophenols

3.3.1 Direct photolysis of nitrophenols

The spectral change of a 4NC solution during a direct photolysis experiment is shown in Fig. 6, color-coded by illumination time, with the inset illustrating the change at different illumination times. The change exhibits wavelength dependence, with a decrease in absorption between 300 and 380 nm but an increase in absorption at 260 nm and above 400 nm. The spectral change is likely due to a combination of 4NC decay and formation of one or more reaction products. Similar trends were also observed for 4NP and 5NG (Sect. S4). The most noteworthy observation for all the nitrophenols is a photo-enhancement of absorption at wavelengths longer than 400 nm, i.e., in the visible range. Since
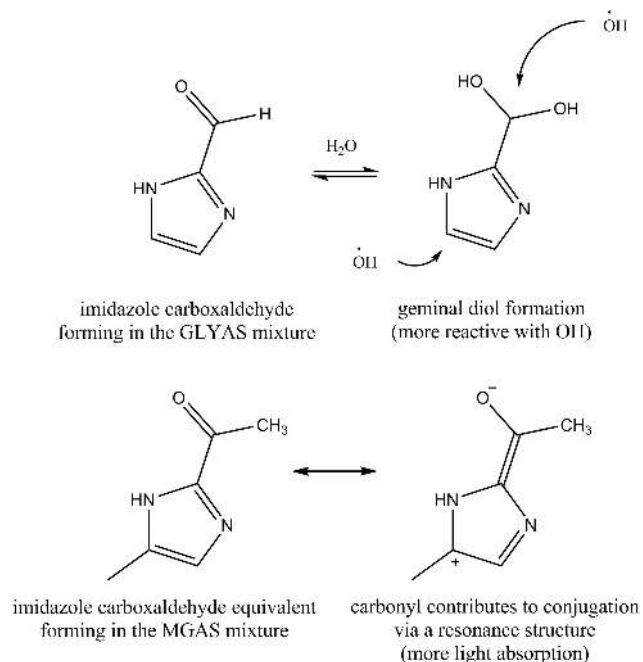
Figure 5. Proposed explanation for the difference in the major bleaching processes of the GLYAS and MGAS solutions.
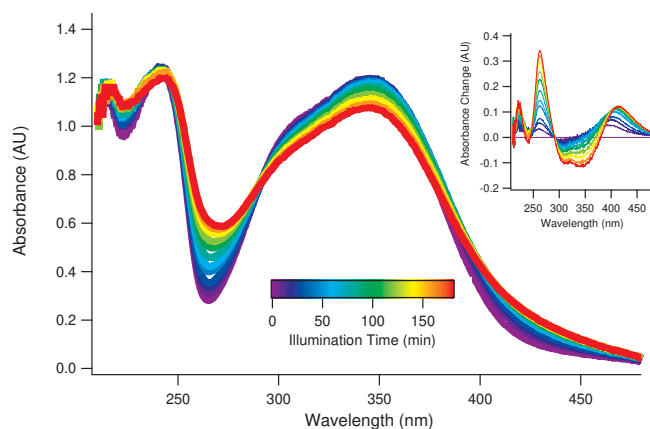

Figure 6. Spectral change of a 4NC solution (4 μM) during a direct photolysis experiment. The inset shows the absorbance change compared to the initial condition.

Figure 7. Time profiles of 4NC absorbance at 420 nm during direct photolysis experiments. Experiments were performed at three solution pH values. An OH scavenger experiment was also performed by adding 1 mM glyoxal to the pH 5 solution.

the photo-enhancement at 420 nm was the most significant for all three nitrophenols, we conducted a series of experiments to better characterize the absorbance change at this wavelength. Formation of color at 420 nm is first order with respect to the precursor nitrophenols, confirmed by altering their concentrations. The discussion below is primarily based on the results from 4NC, while the results of 4NP and 5NG are included in Sect. S5.

The effect of OH radicals is examined first. Previous studies have shown that nitrite ions can be produced during UV irra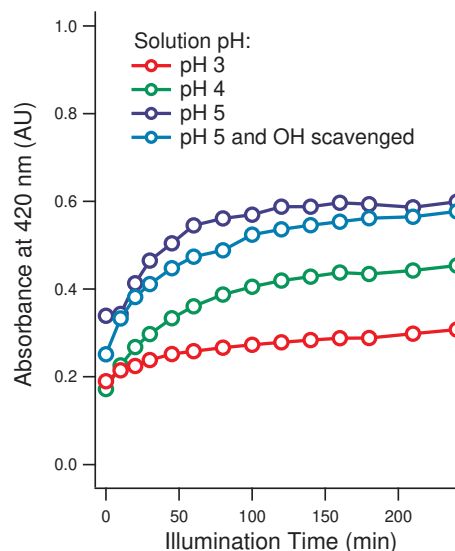diation of nitro-aromatic compounds, via photo-induced nucleophilic substitution reactions (Nakagawa and Crosby, 1974; Dubowski and Hoffmann, 2000; Chen et al., 2005). Nitrite is a photolytic source of OH radicals and can potentially affect our direct photolysis experiments. We performed experiments with 1 mM of glyoxal added to the nitrophenol solution as an OH scavenger. Glyoxal is a good scavenger because neither it nor its reaction products absorb in the wavelength range of interest. Judging from the OH reactivity of nitrophenols (Einschlag et al., 2003) and glyoxal (Tan et al., 2009), 1 mM of glyoxal will scavenge at least 90 % of OH radicals in the solution. The result of a 4NC experiment with an OH scavenger is shown as the cyan trace in Fig. 7, which does not exhibit a significant difference from the experiment without the OH scavenger (blue trace). For 4NP, the OH scavenger reduced but did not completely remove the color formation at 420 nm (Sect. S5). We conclude that photo-enhancement is indeed induced by direct photolysis, even without OH radicals present.

Effects of the solution pH are also examined because the light absorption of phenolic compounds is pH dependent, with phenolate being a better absorber than phenol. Phenolate contains additional lone-pair electrons that can participate in the conjugation system, leading to more efficient light absorption. The absorption spectra of the three nitrophenols at various solution pH values are shown in Sect. S6. Light absorption of 4NP and 4NC at 420 nm increased significantly at higher solution pH due to formation of phenolate, but 5NG did not exhibit pH dependence. A meta-nitrophenol compound, such as 5NG, is known to be less acidic than para- and ortho-nitrophenols (i.e., 4NP and 4NC). It is likely that

Table 2. Rate constants for photo-enhancement at 420 nm for 4-nitrocatechol (4NC).

$k_{\text{direct}}^{\text{I}}$ (s^{-1})			
pH 3	pH 4	pH 5	pH 5 OH scav.
2.3×10^{-4}	3.2×10^{-4}	4.0×10^{-4}	3.3×10^{-4}

the 5NG phenolate did not form in the range of pH investigated.

The absorbance (420 nm) time profiles of 4NC at two additional solution pH (i.e., pH 4 and 3) are displayed in Fig. 7. The photo-enhancement is more significant at higher solution pH. This is perhaps due to the fact that the products formed also exhibit pH-dependent light absorptivity. 4NP and 5NG exhibit unique trends of pH dependence as shown in Sect. S5.

We determined the effective first-order rate coefficient of photo-enhancement ($k_{\text{direct}}^{\text{I}}$) for 4NC by fitting the observed absorbance at 420 nm to a first-order growth curve. The $k_{\text{direct}}^{\text{I}}$ values determined for 4NC are summarized in Table 2. Photo-enhancement in the cases of 4NP and 5NG exhibited stronger linearity, which made fitting to a first-order growth curve difficult. Instead of $k_{\text{direct}}^{\text{I}}$, we report an absorbance-based rate constant for these two compounds, and the details are provided in Sect. S5.

3.3.2 OH oxidation of nitrophenols

Oxidation by OH radicals induced rapid bleaching of all nitrophenols investigated, but the decay of absorbance was not monotonous. The spectral change of 4NC during an OH oxidation experiment is shown in Fig. 8a, while the time profile of absorbance at 420 nm is shown in Fig. 8b. Results for 4NP and 5NG can be found in Sect. S7. All the experiments were performed at pH 5 and in duplicate to confirm reproducibility. For all three nitrophenols investigated, the absorbance exhibited initial increase, followed by decay at longer illumination time.

The initial color formation observed in the current study exhibits similarities to several previous investigations of BB BrC. Gelencser et al. (2003) and Chang and Thompson (2010) have observed color formation in aqueous-phase OH oxidation of aromatic compounds. Saleh et al. (2013) have observed light-absorbing SOA arising from BB particles photochemically aged in a chamber. More recently, Zhong and Jang (2014) have observed a highly dynamic evolution of the optical properties of BB particles, similar to observations from the current study. In their study, the light absorption of BB particles in an outdoor chamber exhibited initial enhancement and subsequent bleaching with exposure to natural sunlight. It is likely that the magnitude of photo-enhancement and bleaching is dependent on both the BrC components and the extent of photochemical processing. Given that nitrophenol presents only a subset of colored components in BB BrC,
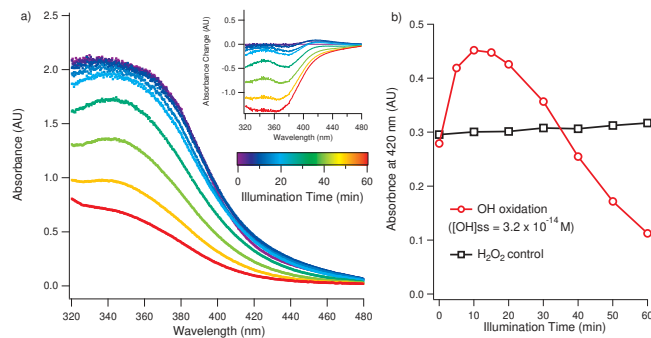
Figure 8. Spectral change of 4NC solution (10 µM) during an OH oxidation experiment **(a)**, with the inset showing absorbance change compared to the initial condition. The color coding represents the illumination time. The time profiles of absorbance at 420 nm are shown in **(b)**.

we cannot draw conclusions on the general fate of BB BrC. As will be seen in Sect. 3.4, WSOC from real BB particles indeed shows complicated results, with different samples exhibiting different trends during direct photolysis.

We propose that the observed trend during OH oxidation is due to initial functionalization followed by ring-cleavage reactions. Previous studies (Sun et al., 2010) have shown that OH oxidation leads to hydroxylation of the aromatic ring, in analogy to the gas phase (Atkinson, 1990). The additional hydroxyl group is electron donating, with its lone-pair electrons contributing to the conjugation and leading to enhanced absorption. We note that oligomeric products have also been reported from OH oxidation of phenolic compounds (Sun et al., 2010; Chang and Thompson, 2010). In particular, Chang and Thompson have observed significant enhancement of absorption, and they proposed that the absorption is attributed to HULIS produced from phenol OH oxidation. To simulate cloudwater chemistry, we used nitrophenol concentrations orders of magnitude lower than those used in Chang and Thompson, and so we consider the formation of oligomers to be less important in our system.

To quantitatively assess the formation and decay rate of color, we applied a kinetic model framework based on the absorbance at 420 nm (Fig. 9a). The OH radical concentration is assumed to be in steady state at 3.2×10^{-13} M, which is the average of measured [OH]ss using the Aerosol-CIMS method. The nitrophenol precursor (NP) follows a prescribed pseudo first-order decay with a rate constant, k_{NP}^{I}, which is estimated based on 4NP OH reactivity reported by Einschlag et al. (2003). A colored product (CP) is formed from NP with a pseudo first-order rate constant $k_{\text{color}}^{\text{I}}$, but simultaneously undergoes photo-bleaching with another pseudo first-order rate constant $k_{\text{bleach}}^{\text{I}}$. Although NP can likely give rise to more than one CP species, the colored products are lumped into a single compound for simplicity. The sum of absorbance from NP and CP is treated as the total absorbance of the solution. We found the optimal combination of $k_{\text{color}}^{\text{I}}$ and $k_{\text{bleach}}^{\text{I}}$

Table 3. Photo-enhancement and bleaching rate constants for nitrophenol OH oxidation determined from a simple kinetic model (Sect. 3.3.2). Note that the rate constants are absorbance-based and should be distinguished from concentration-based rate constants. Values reported here are the average of two replicates.

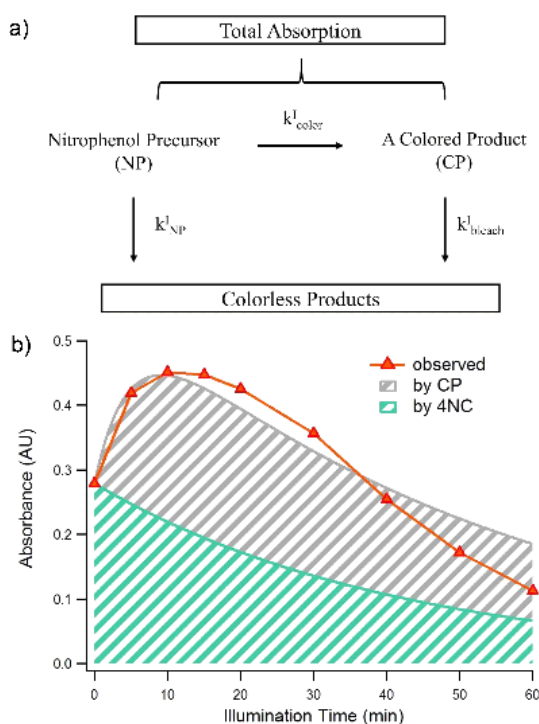| Compound	k_{color}^{I} (s^{-1})	k_{color}^{II} (M^{-1} s^{-1})	k_{bleach}^{I} (s^{-1})	k_{bleach}^{II} (M^{-1} s^{-1})
4-nitrophenol	8.5×10^{-4}	2.6×10^{10}	3.8×10^{-4}	1.2×10^{10}
5-nitroguaiacol	3.9×10^{-3}	1.2×10^{11}	2.0×10^{-3}	6.1×10^{10}
4-nitrocatechol	3.3×10^{-3}	1.0×10^{11}	4.6×10^{-3}	1.4×10^{11}

Figure 9. A schematic illustration of the simple kinetic model **(a)** and one example of 4NC photooxidation **(b)**. The shaded areas in **(b)** are the contributions from a newly formed colored product (CP) and the decaying 4NC, respectively. The red line follows data from an experiment.

values that minimizes the sum of the squared difference between the modeled and observed absorbance changes. We note that k_{color}^{I} and k_{bleach}^{I} are absorbance-based rate constants and should not be confused with concentration-based rate constants. If the identity and molar absorptivity of CP are characterized in future studies, these absorbance-based rate constants can be converted into concentration basis.

The results for one 4NC experiment are shown in Fig. 9b. The two shaded areas in Fig. 9b represent modeled absorbance due to the precursor, 4NC, and the CP, respectively. The red trace is the absorbance change during the experiment shown in Fig. 8. Results for 4NP and 5NG, along with detailed model conditions, are included in Sect. S8. For all three nitrophenols, this model captures the initial increase

and later decay of color, but the time at which the absorbance reaches its maximum and the decay rate at the end of the experiment are more difficult to match. This is perhaps due to the fact that nitrophenols form multiple generations of colored products, giving rise to a more dynamic evolution of absorbance than the current model framework can produce. Nevertheless, the model represents a novel effort to estimate the rates of photo-enhancement and bleaching during OH oxidation of nitrophenols. The optimal k_{color}^{I} and k_{bleach}^{I} values for the three nitrophenols are listed in Table 3. Since these values are all pseudo-first-order rate constants, their corresponding second-order rate constants (k_{color}^{II} and k_{bleach}^{II}) are also calculated using Eq. (2) and provided in Table 3. The values reported in Table 3 are the average of two replicates performed for each nitrophenol. Relative errors are roughly 10 % for 4NP and 5NG, and 15 % for 4NC.

3.3.3 Atmospheric fate of nitrophenols

Our results indicate that the photo-bleaching by OH oxidation is rapid and presents the dominant fate for BrC represented by nitrophenols. As the [OH]ss in our experiment (3.2×10^{-14} M) is roughly that of cloudwater in remote areas (Herrmann et al., 2010), the light absorptivity of nitrophenols is expected to reach its maxima and to be bleached within 1 h of in-cloud time. On the other hand, photo-enhancement during direct photolysis is much slower, with color forming over a timescale of hours. This observation agrees with Vione et al. (2009), where they also determined radical chemistry to be the dominant sink of 4NP compared to direct photolysis. That being said, this trend may not apply to all nitrophenols. For instance, dinitrophenols represent an interesting group of compounds to investigate in the future, as the additional nitro group deactivates OH radical reactions (Einschlag et al., 2003) but enhances light absorption (Schwarzenbach et al., 1988).

3.3.4 Direct photolysis of WSOC frombiofuel combustion samples

A change in absorptivity was observed when WSOC from biofuel combustion samples was exposed to simulated sunlight. Results for the kaoliang stalk sample and the cotton stalk sample are shown in Fig. 10a and b, respectively. Their absorbance changes at three wavelengths (350,
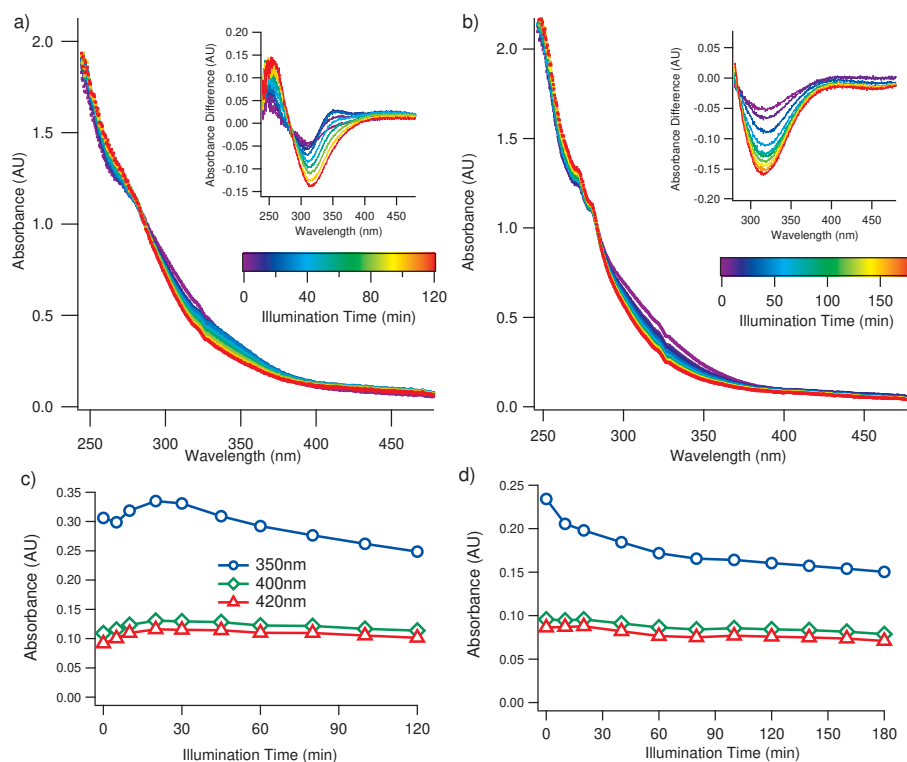
Figure 10. Direct photolysis of the WSOC from biofuel combustion samples. The spectral evolution of the kaoliang and the cotton samples is shown in **(a)** and **(b)**, respectively. The color code indicates illumination time, while the insets show the absorbance change compared to the initial condition. The time profiles of absorbance at three different wavelengths for the same samples are shown in **(c)** and **(d)**, respectively.

400 and 420 nm) are also shown in Fig. 10c and d, respectively. WSOC from the two samples exhibited different trends, with the kaoliang stalk sample showing a temporary photo-enhancement shortly after the initiation of illumination, and the cotton stalk sample exhibiting monotonous photo-bleaching. The trends for the sample at different wavelengths demonstrate the complexity of the real biomass burning samples. Our results provide qualitative evidence that the optical properties of WSOC extracted from BB BrC can change upon photochemistry.

4   Conclusions and atmospheric implications

The overall conclusion from this work is that, because atmospheric brown carbon species are organic chromophores and susceptible to photochemical degradation, their optical properties are altered by aqueous-phase photochemical processing with both photo-enhancement and photo-bleaching possibly occurring. In particular, imine-mediated BrC, arising from aqueous-phase reactions between carbonyl compounds and nitrogen-containing nucleophiles, undergoes rapid photo-bleaching via both direct photolysis and OH oxidation. Such rapid photo-bleaching may indicate a reason why Imine BrC has not yet been observed in ambient samples. Bleaching of glyoxal–ammonium sulfate (GLYAS) BrC

was predominantly driven by OH oxidation, whereas that for methylglyoxal–ammonium sulfate (MGAS) was driven by direct photolysis. Three species of nitrophenols were investigated as an important subset of biomass burning BrC. Photo-enhancement of absorption was observed when the nitrophenol species are illuminated with simulated sunlight, as well as during the initial stages of OH oxidation. Although such photo-enhancement can potentially magnify the direct radiative effect of nitrophenols, photo-bleaching of nitrophenols with further OH exposure was observed to be also rapid. This is the first investigation of OH oxidation-induced effects on the optical properties of BrC, demonstrating its importance in determining the atmospheric significance of BrC. Lastly, a study of biofuel BrC species illustrated that the optical properties of ambient samples are also rapidly altered. These findings are in general agreement with prior studies that have also seen evidence for photo-bleaching (Lee et al., 2014b; Zhong and Jang, 2014; Sareen et al., 2013).

Using atmospherically relevant light levels and aqueous OH concentrations, the timescales for these changes are all rapid, i.e., on the order of an hour or less. This indicates that the atmospheric concentrations of BrC species will be highest during the night, when their atmospheric significance for shortwave radiative forcing is zero. For example, in the case of the Imine BrC species, they may form slowly during

the night in cloudwater or aerosol water and then will decay away rapidly in the morning. It is expected that, during the daytime, their steady state concentrations will be highest in regions where there is considerable droplet evaporation proceeding. Biomass burning BrC emitted during the nighttime will be stable. Upon sunrise, photochemistry can induce photo-enhancement, but the BrC concentration will also fall with further photochemical processing. The magnitude of photo-enhancement and bleaching is likely dependent on the BrC components, as well as OH exposure. We conclude that atmospheric models that include only source functions and depositional loss rates for BrC-bearing organic aerosol will misrepresent the radiative impacts of these particles, requiring additional parameterizations for photo-bleaching and photo-enhancement.

While this study provides fundamental information on the behavior of BrC during photochemical processing, it is also subject to several limitations. Choices of a few single BrC species may limit the atmospheric implications one can make from this study. As the trends observed in the WSOC of biofuel combustion samples are distinct from those observed in Imine BrC and nitrophenols (see Sect. 3.4), the current study also illustrates the importance for a more systematic investigation for ambient BrC from different origins. The kinetic information obtained from this study is based on the changes in the bulk light absorptivity. Molecular-level investigations should be performed in the future to convert the absorbance-based rate coefficients into concentration-based ones. Whereas this paper has focused upon aqueous-phase processing of water-soluble BrC, a significant fraction of BrC is water-insoluble (Chen and Bond, 2010; Zhang et al., 2013; Washenfelder et al., 2015), with heterogeneous oxidation likely affecting its atmospheric lifetime. It will be important to also assess the rates of heterogeneous oxidation of BrC species in particles via interactions with gas-phase oxidants and to study direct photolysis in aerosol particles.

The Supplement related to this article is available online at doi:10.5194/acp-15-6087-2015-supplement.

References

Alexander, D. T., Crozier, P. A., and Anderson, J. R.: Brown carbon spheres in East Asian outflow and their optical properties, Science, 321, 833–836, 2008.

Aljawhary, D., Lee, A. K. Y., and Abbatt, J. P. D.: High-resolution chemical ionization mass spectrometry (ToF-CIMS): application to study SOA composition and processing, Atmos. Meas. Tech., 6, 3211–3224, doi:10.5194/amt-6-3211-2013, 2013.

Andreae, M. O. and Gelencsér, A.: Black carbon or brown carbon? The nature of light-absorbing carbonaceous aerosols, Atmos. Chem. Phys., 6, 3131–3148, doi:10.5194/acp-6-3131-2006, 2006.

Aregahegn, K. Z., Noziere, B., and George, C.: Organic aerosol formation photo-enhanced by the formation of secondary photosensitizers in aerosols, Faraday Discussions, 165, 123–134, 2013.

Atkinson, R.: Gas-Phase Tropospheric Chemistry of Organic-Compounds]- a Review, Atmos. Environ. A-Gen., 24, 1–41, 1990.

Bahadur, R., Praveen, P. S., Xu, Y., and Ramanathan, V.: Solar absorption by elemental and brown carbon determined from spectral observations, P. Natl. Acad. Sci., 109, 17366–17371, 2012.

Blando, J. D. and Turpin, B. J.: Secondary organic aerosol formation in cloud and fog droplets: a literature evaluation of plausibility, Atmos. Environ., 34, 1623–1632, 2000.

Bond, T. C.: Spectral dependence of visible light absorption by carbonaceous particles emitted from coal combustion, Geophys. Res. Lett., 28, 4075–4078, 2001.

Bones, D. L., Henricksen, D. K., Mang, S. A., Gonsior, M., Bateman, A. P., Nguyen, T. B., Cooper, W. J., and Nizkorodov, S. A.: Appearance of strong absorbers and fluorophores in limonene-O_3 secondary organic aerosol due to NH_{4+}-mediated chemical aging over long time scales, J. Geophys. Res.-Atmos. (1984–2012), 115, 2010.

Chan, T. W., Huang, L., Leaitch, W. R., Sharma, S., Brook, J. R., Slowik, J. G., Abbatt, J. P. D., Brickell, P. C., Liggio, J., Li, S.-M., and Moosmüller, H.: Observations of OM/OC and specific attenuation coefficients (SAC) in ambient fine PM at a rural site in central Ontario, Canada, Atmos. Chem. Phys., 10, 2393–2411, doi:10.5194/acp-10-2393-2010, 2010.

Chang, J. L. and Thompson, J. E.: Characterization of colored products formed during irradiation of aqueous solutions containing H_2O_2 and phenolic compounds, Atmos. Environ., 44, 541–551, 2010.

Chen, B., Yang, C., and Goh, N. K.: Direct photolysis of nitroaromatic compounds in aqueous solutions, J. Environ. Sci., 17, 598–604, 2005.

Chen, Y. and Bond, T. C.: Light absorption by organic carbon from wood combustion, Atmos. Chem. Phys., 10, 1773–1787, doi:10.5194/acp-10-1773-2010, 2010.

Chung, S. H. and Seinfeld, J. H.: Global distribution and climate forcing of carbonaceous aerosols, J. Geophys. Res.-Atmos., 107, D19107, doi:10.1029/2001JD001397, 2002.

De Haan, D. O., Corrigan, A. L., Smith, K. W., Stroik, D. R., Turley, J. J., Lee, F. E., Tolbert, M. A., Jimenez, J. L., Cordova, K. E., and Ferrell, G. R.: Secondary organic aerosol-forming reactions of glyoxal with amino acids, Environ. Sci. Technol., 43, 2818–2824, 2009.

De Haan, D. O., Hawkins, L. N., Kononenko, J. A., Turley, J. J., Corrigan, A. L., Tolbert, M. A., and Jimenez, J. L.: Formation of

nitrogen-containing oligomers by methylglyoxal and amines in simulated evaporating cloud droplets, Environ. Sci. Technol., 45, 984–991, 2010.

Desyaterik, Y., Sun, Y., Shen, X., Lee, T., Wang, X., Wang, T., and Collett, J. L.: Speciation of brown carbon in cloud water impacted by agricultural biomass burning in eastern China, J. Geophys. Res.- Atmos., 118, 7389–7399, 2013.

Dubowski, Y. and Hoffmann, M. R.: Photochemical transformations in ice: Implications for the fate of chemical species, Geophys. Res. Lett., 27, 3321–3324, 2000.

Einschlag, F. S. G., Carlos, L., and Capparelli, A. L.: Competition kinetics using the UV/H_2O_2 process: a structure reactivity correlation for the rate constants of hydroxyl radicals toward nitroaromatic compounds, Chemosphere, 53, 1–7, 2003.

Einschlag, F. S. G., Felice, J. I., and Triszcz, J. M.: Kinetics of nitrobenzene and 4-nitrophenol degradation by UV irradiation in the presence of nitrate and nitrite ions, Photoch. Photobio. Sci., 8, 953–960, 2009.

Ervens, B., Turpin, B. J., and Weber, R. J.: Secondary organic aerosol formation in cloud droplets and aqueous particles (aqSOA): a review of laboratory, field and model studies, Atmos. Chem. Phys., 11, 11069–11102, doi:10.5194/acp-11-11069-2011, 2011.

Feng, Y., Ramanathan, V., and Kotamarthi, V. R.: Brown carbon: a significant atmospheric absorber of solar radiation?, Atmos. Chem. Phys., 13, 8607–8621, doi:10.5194/acp-13-8607-2013, 2013.

Flores, J., Washenfelder, R., Adler, G., Lee, H., Segev, L., Laskin, J., Laskin, A., Nizkorodov, S., Brown, S., and Rudich, Y.: Complex refractive indices in the near-ultraviolet spectral region of biogenic secondary organic aerosol aged with ammonia, Phys. Chem. Chem. Phys., 16, 10629–10642, 2014.

Galbavy, E. S., Ram, K., and Anastasio, C.: 2-Nitrobenzaldehyde as a chemical actinometer for solution and ice photochemistry, J. Photoch. Photobio. A, 209, 186–192, 2010.

Galloway, M. M., Powelson, M. H., Sedehi, N., Wood, S. E., Millage, K. D., Kononenko, J. A., Rynaski, A. D., and De Haan, D. O.: Secondary Organic Aerosol Formation during Evaporation of Droplets Containing Atmospheric Aldehydes, Amines, and Ammonium Sulfate, Environ. Sci. Technol., 48, 14417–14425, 2014.

Gelencser, A., Hoffer, A., Kiss, G., Tombacz, E., Kurdi, R., and Bencze, L.: In-situ formation of light-absorbing organic matter in cloud water, J. Atmos. Chem., 45, 25–33, 2003.

Graber, E. R. and Rudich, Y.: Atmospheric HULIS: How humic-like are they? A comprehensive and critical review, Atmos. Chem. Phys., 6, 729–753, doi:10.5194/acp-6-729-2006, 2006.

Harrison, M. A., Barra, S., Borghesi, D., Vione, D., Arsene, C., and Olariu, R. I.: Nitrated phenols in the atmosphere: a review, Atmos. Environ., 39, 231–248, 2005.

Herrmann, H., Hoffmann, D., Schaefer, T., Braeuer, P., and Tilgner, A.: Tropospheric Aqueous-Phase Free-Radical Chemistry: Radical Sources, Spectra, Reaction Kinetics and Prediction Tools, Chemphyschem, 11, 3796–3822, 2010.

Hoffer, A., Kiss, G., Blazso, M., and Gelencser, A.: Chemical characterization of humic-like substances (HULIS) formed from a lignin-type precursor in model cloud water, Geophys. Res. Lett., 31, L06115, doi:10.1029/2003GL018962, 2004.

Hoffmann, D., Weigert, B., Barzaghi, P., and Herrmann, H.: Reactivity of poly-alcohols towards OH, NO_3 and SO_4^- in aqueous solution, Phys. Chem. Chem. Phys., 11, 9351–9363, 2009.

Huang, L., Brook, J., Zhang, W., Li, S., Graham, L., Ernst, D., Chivulescu, A., and Lu, G.: Stable isotope measurements of carbon fractions (OC/EC) in airborne particulate: A new dimension for source characterization and apportionment, Atmos. Environ., 40, 2690–2705, 2006.

Iinuma, Y., Bruggemann, E., Gnauk, T., Muller, K., Andreae, M., Helas, G., Parmar, R., and Herrmann, H.: Source characterization of biomass burning particles: the combustion of selected European conifers, African hardwood, savanna grass, and German and Indonesian peat, J. Geophys. Res.-Atmos., 112, D08209, doi:10.1029/2006JD007120, 2007.

Iinuma, Y., Boge, O., Grafe, R., and Herrmann, H.: Methyl-nitrocatechols: atmospheric tracer compounds for biomass burning secondary organic aerosols, Environ. Sci. Technol., 44, 8453–8459, 2010.

Jacobson, M. Z.: Isolating nitrated and aromatic aerosols and nitrated aromatic gases as sources of ultraviolet light absorption, J. Geophys. Res.-Atmos., 104, 3527–3542, 1999.

Kampf, C. J., Jakob, R., and Hoffmann, T.: Identification and characterization of aging products in the glyoxal/ammonium sulfate system – implications for light-absorbing material in atmospheric aerosols, Atmos. Chem. Phys., 12, 6323–6333, doi:10.5194/acp-12-6323-2012, 2012.

Kirchstetter, T. W. and Thatcher, T. L.: Contribution of organic carbon to wood smoke particulate matter absorption of solar radiation, Atmos. Chem. Phys., 12, 6067–6072, doi:10.5194/acp-12-6067-2012, 2012.

Kirchstetter, T. W., Novakov, T., and Hobbs, P. V.: Evidence that the spectral dependence of light absorption by aerosols is affected by organic carbon, J. Geophys. Res.-Atmos., 109, D21208, doi:10.1029/2004JD004999, 2004.

Kitanovski, Z., Irena, G., Vermeylen, R., Claeys, M., and Maenhaut, W.: Liquid chromatography tandem mass spectrometry method for characterization of monoaromatic nitro-compounds in atmospheric particulate matter, J. Chromatogr. A, 1268, 35–43, 2012.

Knopf, D. A., Forrester, S. M., and Slade, J. H.: Heterogeneous oxidation kinetics of organic biomass burning aerosol surrogates by O_3, NO_2, N_2O_5, and NO_3, Phys. Chem. Chem. Phys., 13, 21050–21062, 2011.

Lack, D. A., Langridge, J. M., Bahreini, R., Cappa, C. D., Middlebrook, A. M., and Schwarz, J. P.: Brown carbon and internal mixing in biomass burning particles, P. Natl. Acad. Sci., 109, 14802–14807, 2012.

Laskin, A., Laskin, J., and Nizkorodov, S. A.: Chemistry of Atmospheric Brown Carbon, Chem. Rev., 115, 4335–4382, doi:10.1021/cr5006167, 2015.

Laskin, J., Laskin, A., Nizkorodov, S. A., Roach, P., Eckert, P., Gilles, M. K., Wang, B., Lee, H. J., and Hu, Q.: Molecular Selectivity of Brown Carbon Chromophores, Environ. Sci. Technol., 48, 12047–12055, 2014.

Lee, A. K., Zhao, R., Li, R., Liggio, J., Li, S.-M., and Abbatt, J. P.: Formation of light absorbing organo-nitrogen species from evaporation of droplets containing glyoxal and ammonium sulfate, Environ. Sci. Technol., 47, 12819–12826, 2013.

Lee, B. H., Lopez-Hilfiker, F., Mohr, C., Kurten, T. C., Worsnop, D., and Thornton, J. A.: An iodide-adduct high-resolution time-of-

flight chemical-ionization mass spectrometer: application to atmospheric inorganic and organic compounds, Environ. Sci. Technol., 48, 6309–6317, 2014a.

Lee, H. J., Aiona, P. K., Laskin, A., Laskin, J., and Nizkorodov, S. A.: Effect of solar radiation on the optical properties and molecular composition of laboratory proxies of atmospheric brown carbon, Environ. Sci. Technol., 48, 10217–10226, 2014b.

Li, X., Duan, L., Wang, S., Duan, J., Guo, X., Yi, H., Hu, J., Li, C., and Hao, J.: Emission characteristics of particulate matter from rural household biofuel combustion in China, Energy Fuels, 21, 845–851, 2007.

Li, X., Wang, S., Duan, L., Hao, J., and Nie, Y.: Carbonaceous aerosol emissions from household biofuel combustion in China, Environ. Sci. Technol., 43, 6076–6081, 2009.

Lin, G., Penner, J. E., Flanner, M. G., Sillman, S., Xu, L., and Zhou, C.: Radiative forcing of organic aerosol in the atmosphere and on snow: effects of SOA and brown carbon, J. Geophys. Res.-Atmos., 119, 7453–7476, doi:10.1002/2013JD021186, 2014.

Liu, J., Scheuer, E., Dibb, J., Ziemba, L. D., Thornhill, K., Anderson, B. E., Wisthaler, A., Mikoviny, T., Devi, J. J., Bergin, M., and Weber, R. J.: Brown carbon in the continental troposphere, Geophys. Res. Lett., 41, 2191–2195, 2014.

Luttke, J. and Levsen, K.: Phase partitioning of phenol and nitrophenols in clouds, Atmos. Environ., 31, 2649–2655, 1997.

Luttke, J., Levsen, K., Acker, K., Wieprecht, W., and Moller, D.: Phenols and nitrated phenols in clouds at Mount Brocken, Int. Environ. An. Ch., 74, 69–89, 1999.

Mohr, C., Lopez-Hilfiker, F. D., Zotter, P., Prevot, A. S., Xu, L., Ng, N. L., Herndon, S. C., Williams, L. R., Franklin, J. P., Zahniser, M. S., Worsnop, D. R., Knighton, W. B., Aiken, A. C., Gorkowski, K. J., Dubey, M. K., Allan, J. D., and Thornton, J. A.: Contribution of nitrated phenols to wood burning brown carbon light absorption in Detling, UK during winter time, Environ. Sci. Technol., 47, 6316–6324, 2013.

Monod, A., Poulain, L., Grubert, S., Voisin, D., and Wortham, H.: Kinetics of OH-initiated oxidation of oxygenated organic compounds in the aqueous phase: new rate constants, structure-activity relationships and atmospheric implications, Atmos. Environ., 39, 7667–7688, 2005.

Nakagawa, M. and Crosby, D. G.: Photodecomposition of nitrofen, J. Agr. Food Chem., 22, 849–853, 1974.

Nguyen, T. B., Lee, P. B., Updyke, K. M., Bones, D. L., Laskin, J., Laskin, A., and Nizkorodov, S. A.: Formation of nitrogen- and sulfur-containing light-absorbing compounds accelerated by evaporation of water from secondary organic aerosols, J. Geophys. Res.-Atmos., 117, 2012.

Nguyen, T. B., Laskin, A., Laskin, J., and Nizkorodov, S. A.: Brown carbon formation from ketoaldehydes of biogenic monoterpenes, Faraday Discussions, 165, 473–494, 2013.

Noziere, B., Dziedzic, P., and Cordova, A.: Products and Kinetics of the Liquid-Phase Reaction of Glyoxal Catalyzed by Ammonium Ions (NH_4^+), J. Phys. Chem., 113, 231–237, 2009.

Petters, M. D. and Kreidenweis, S. M.: A single parameter representation of hygroscopic growth and cloud condensation nucleus activity, Atmos. Chem. Phys., 7, 1961–1971, doi:10.5194/acp-7-1961-2007, 2007.

Petters, M. D., Carrico, C. M., Kreidenweis, S. M., Prenni, A. J., DeMott, P. J., Collett, J. L., and Moosmuller, H.: Cloud condensation nucleation activity of biomass burning aerosol, J. Geophys. Res.-Atmos., 114, D22205, doi:10.1029/2009JD012353, 2009.

Phillips, S. M. and Smith, G. D.: Light absorption by charge transfer complexes in brown carbon aerosols, Environ. Sci. Technol. Lett., 1, 382–386, 2014.

Powelson, M. H., Espelien, B. M., Hawkins, L. N., Galloway, M. M., and Haan, D. O. D.: Brown carbon formation by aqueous-phase carbonyl compound reactions with amines and ammonium sulfate, Environ. Sci. Technol., 48, 985–993, 2013.

Saleh, R., Hennigan, C. J., McMeeking, G. R., Chuang, W. K., Robinson, E. S., Coe, H., Donahue, N. M., and Robinson, A. L.: Absorptivity of brown carbon in fresh and photo-chemically aged biomass-burning emissions, Atmos. Chem. Phys., 13, 7683–7693, doi:10.5194/acp-13-7683-2013, 2013.

Saleh, R., Robinson, E. S., Tkacik, D. S., Ahern, A. T., Liu, S., Aiken, A. C., Sullivan, R. C., Presto, A. A., Dubey, M. K., Yokelson, R. J., Donahue, N. M., and Robinson, A. L.: Brownness of organics in aerosols from biomass burning linked to their black carbon content, Nat. Geosci., 7, 647–650, 2014.

Sareen, N., Schwier, A. N., Shapiro, E. L., Mitroo, D., and McNeill, V. F.: Secondary organic material formed by methylglyoxal in aqueous aerosol mimics, Atmos. Chem. Phys., 10, 997–1016, doi:10.5194/acp-10-997-2010, 2010.

Sareen, N., Moussa, S. G., and McNeill, V. F.: Photochemical aging of light-absorbing secondary organic aerosol material, J. Phys. Chem. A, 117, 2987–2996, 2013.

Schwarzenbach, R. P., Stierli, R., Folsom, B. R., and Zeyer, J.: Compound properties relevant for assessing the environmental partitioning of nitrophenols, Environ. Sci. Technol., 22, 83–92, 1988.

Sedehi, N., Takano, H., Blasic, V. A., Sullivan, K. A., and Haan, D. O. D.: Temperature-and pH-dependent aqueous-phase kinetics of the reactions of glyoxal and methylglyoxal with atmospheric amines and ammonium sulfate, Atmos. Environ., 77, 656–663, 2013.

Shapiro, E. L., Szprengiel, J., Sareen, N., Jen, C. N., Giordano, M. R., and McNeill, V. F.: Light-absorbing secondary organic material formed by glyoxal in aqueous aerosol mimics, Atmos. Chem. Phys., 9, 2289–2300, doi:10.5194/acp-9-2289-2009, 2009.

Slade, J. H. and Knopf, D. A.: Multiphase OH oxidation kinetics of organic aerosol: The role of particle phase state and relative humidity, Geophys. Res. Lett., 41, 5297–5306, 2014.

Sun, Y. L., Zhang, Q., Anastasio, C., and Sun, J.: Insights into secondary organic aerosol formed via aqueous-phase reactions of phenolic compounds based on high resolution mass spectrometry, Atmos. Chem. Phys., 10, 4809–4822, doi:10.5194/acp-10-4809-2010, 2010.

Tan, Y., Perri, M. J., Seitzinger, S. P., and Turpin, B. J.: Effects of precursor concentration and acidic sulfate in aqueous glyoxal-oh radical oxidation and implications for secondary organic aerosol, Environmental Science & Technology, 43, 8105–8112, 2009.

Updyke, K. M., Nguyen, T. B., and Nizkorodov, S. A.: Formation of brown carbon via reactions of ammonia with secondary organic aerosols from biogenic and anthropogenic precursors, Atmos. Environ., 63, 22–31, 2012.

Vione, D., Maurino, V., Minero, C., Duncianu, M., Olariu, R.-I., Arsene, C., Sarakha, M., and Mailhot, G.: Assessing the transformation kinetics of 2-and 4-nitrophenol in the atmospheric aque-

ous phase. Implications for the distribution of both nitroisomers in the atmosphere, Atmos. Environ., 43, 2321–2327, 2009.

Washenfelder, R. A., Attwood, A. R., Brock, C. A., Guo, H., Xu, L., Weber, R. J., Ng, N. L., Allen, H. M., Ayres, B. R., Baumann, K., Cohen, R. C., Draper, D. C., Duffey, K. C., Edgerton, E., Fry, J. L., Hu, W. W., Jimenez, J. L., Palm, B. B., Romer, P., Stone, E. A., Wooldridge, P. J., and Brown, S. S.: Biomass burning dominates brown carbon absorption in the rural southeastern United States, Geophys. Res. Lett., 42, 653–664, doi:10.1002/2014GL062444, 2015.

Yu, G., Bayer, A., Galloway, M., Korshavn, K., Fry, C., and Keutsch, F.: Glyoxal in aqueous ammonium sulfate solutions: products, kinetics and hydration effects, Environ. Sci. Technol., 45, 6336–6342, 2011.

Zarzana, K. J., Haan, D. O. D., Freedman, M. A., Hasenkopf, C. A., and Tolbert, M. A.: Optical properties of the products of α-dicarbonyl and amine reactions in simulated cloud droplets, Environ. Sci. Technol., 46, 4845–4851, 2012.

Zhang, X., Lin, Y.-H., Surratt, J. D., Zotter, P., Prévôt, A. S., and Weber, R. J.: Light-absorbing soluble organic aerosol in Los Angeles and Atlanta: A contrast in secondary organic aerosol, Geophys. Res. Lett., 38, 2011.

Zhang, X., Lin, Y.-H., Surratt, J. D., and Weber, R. J.: Sources, composition and absorption Ångstrom exponent of light-absorbing organic components in aerosol extracts from the Los Angeles Basin, Environ. Sci. Technol., 47, 3685–3693, 2013.

Zhao, R., Lee, A. K. Y., and Abbatt, J. P. D.: Investigation of aqueous-phase photooxidation of glyoxal and methylglyoxal by aerosol chemical ionization mass spectrometry: observation of hydroxyhydroperoxide formation, J. Phys. Chem. A, 116, 6253–6263, 2012.

Zhao, R., Mungall, E. L., Lee, A. K. Y., Aljawhary, D., and Abbatt, J. P. D.: Aqueous-phase photooxidation of levoglucosan – a mechanistic study using aerosol time-of-flight chemical ionization mass spectrometry (Aerosol ToF-CIMS), Atmos. Chem. Phys., 14, 9695–9706, doi:10.5194/acp-14-9695-2014, 2014.

Zhao, S., Ma, H., Wang, M., Cao, C., Xiong, J., Xu, Y., and Yao, S.: Study on the mechanism of photo-degradation of p-nitrophenol exposed to 254nm UV light, J. Hazard. Mater., 180, 86–90, 2010.

Zhong, M. and Jang, M.: Dynamic light absorption of biomass-burning organic carbon photochemically aged under natural sunlight, Atmos. Chem. Phys., 14, 1517–1525, doi:10.5194/acp-14-1517-2014, 2014.